Coordination and Conversion of Urea at Dinuclear μ-Acetato Nickel(II) Complexes with Symmetric and Asymmetric Cores

Matthias Konrad, Franc Meyer,* Albrecht Jacobi, Peter Kircher, Peter Rutsch, and Laszlo Zsolnai

Anorganisch-Chemisches Institut der Universität Heidelberg, Im Neuenheimer Feld 270, D-69120 Heidelberg, Germany

Received February 1, 1999

A series of symmetric and asymmetric pyrazolate-based dinuclear Ni(II) complexes relevant to the active site of urease is reported, which have acetate ions as secondary bridges and which feature variations in the type (N or S) and number of donor sites provided within the individual coordination compartments of the primary pyrazolate ligand matrixes. X-ray crystallographic structures of the acetone adduct $[L^1Ni_2(\mu\text{-OAc})(\text{acetone})_2](ClO_4)_2$ (**1**) as well as of the urea adducts $[L^1Ni_2(\mu\text{-OAc})(\text{benzylurea})_2](ClO_4)_2$ (**2c**), $[L^2Ni_2(\mu\text{-OAc})(\text{urea})](ClO_4)_2$ (**3a**), and $[L^3Ni_2(\mu\text{-OAc})(N,N'\text{-dimethylurea})_2(MeOH)_2](ClO_4)_2$ (**4**) have been determined. They reveal that the urea substrates are tied up with the bimetallic cores by both O-coordination to the metal centers and hydrogen bonding between the urea NH and the O atoms of the bridging acetate. In a related complex $[L^3Ni_2(\mu\text{-OAc})(OAc)_2Na]BPh_4$ (**5**) a sodium ion is associated with the dinickel framework via binding to one O atom of each of the three acetates. The nickel(II) ions in **1** and **2a** are weakly antiferromagnetically coupled ($J = -2.6$ and -1.9 cm^{-1}), where the magnitude of the coupling appears to correlate with the tilting of the acetate moiety with respect to the plane of the pyrazolate. The superexchange in **3a** and **4** is even weaker. The ability of the new complexes to mediate the ethanolysis of urea is examined and is found to be dependent on the number and stereochemical arrangement of the accessible coordination sites at the dinuclear core: the asymmetric species **3a** is not capable of inducing any solvolysis of the substrate, and the activity of the symmetric systems **1** and **2b** is less than stoichiometric, whereas **4** displays higher activity, albeit this is still very low and possibly proceeds via a one metal ion mechanism.

Introduction

The nickel-dependent metalloenzyme urease is present in various plants and microorganisms and catalyzes the hydrolysis of urea to ammonia and carbon dioxide.[1] The initial X-ray crystal structure of native urease from *Klebsiella aerogenes* as well as subsequent crystallographic work has provided detailed insights into the active site structure and has identified a pair of nickel ions that are nonequivalent and are found in differing coordination environments at a Ni···Ni separation of 3.5 Å.[2,3] These findings lend further support for the previously suggested catalytic mechanism,[4] which assumes that urea is activated by coordination to one nickel(II) ion and is subsequently attacked by a nucleophilic hydroxide bound to the adjacent nickel center.[5]

Some molecular model systems have been prepared in order to elucidate the possible binding modes of urea as well as to enable hydrolytic transformations at dinuclear nickel(II) cores relevant to the urease enzyme,[6−9] and recently the first catalytic ethanolysis of urea by a (μ-alkoxo)(μ-carboxylato)dinickel(II) complex was reported.[8] Obviously, the resolving of the catalytic pathway of this fascinating metalloenzyme remains a subject of intense research and therefore encourages further efforts to provide analogues of the urease active site and to ultimately exploit and mimic its unique reactivity. In the present contribution we report the synthesis and crystallographic characterization of a series of pyrazolate-based dinickel(II) complexes capable of binding urea. Without trying to exactly reproduce structural characteristics of the native enzyme, these novel systems are designed to differ by the type and number of donor sites of each coordination compartment as well as by the presence of a

* To whom correspondence should be addressed.
† FAX: (0049)-6221-545707. E-mail: Franc@sun0.urz.uni-heidelberg.de.

(1) (a) Halcrow, M. A.; Christou, G. *Chem. Rev.* **1994**, *94*, 2421. (b) Kolodziej, A. F. *Prog. Inorg. Chem.* **1994**, *41*, 493. (c) Maroney, M. J.; Davidson, G.; Allan, C. B.; Figlar, J. *Struct. Bonding* **1998**, *91*, 1. (d) Fonticella-Camps, J. C. *Struct. Bonding* **1998**, *92*, 1.
(2) (a) Jabri, E.; Carr, M. B.; Hausinger, R. P.; Karplus, P. A. *Science* **1995**, *268*, 998. (b) Pearson, M. A.; Michel, L. O.; Hausinger, R. P.; Karplus, P. A. *Biochemistry* **1997**, *36*, 8164.
(3) Karplus, P. A.; Pearson, M. A.; Hausinger, R. P. *Acc. Chem. Res.* **1997**, *30*, 330.
(4) Dixon, N. E.; Riddles, P. W.; Gazzola, C.; Blakeley, R. L.; Zerner, B. *Can. J. Biochem.* **1980**, *58*, 1335.
(5) Lippard, S. J. *Science* **1995**, *268*, 996.
(6) (a) Buchanan, R. M.; Mashuta, M. S.; Oberhausen, K. J.; Richardson, J. F. *J. Am. Chem. Soc.* **1989**, *111*, 4497. (b) Wages, H. E.; Taft, K. L.; Lippard, S. J. *Inorg. Chem.* **1993**, *32*, 4985. (c) Volkmer, D.; Hörstmann, A.; Griesar, K.; Haase, W.; Krebs, B. *Inorg. Chem.* **1996**, *35*, 1132. (d) Volkmer, D.; Hommerich, B.; Griesar, K.; Haase, W.; Krebs, B. *Inorg. Chem.* **1996**, *35*, 3792. (e) Meyer, F.; Jacobi, A.; Nuber, B.; Rutsch, P.; Zsolnai, L. *Inorg. Chem.* **1998**, *37*, 1213. (f) Koga, T.; Furutachi, H.; Nakamura, T.; Fukita, N.; Ohba, M.; Takahashi, K.; Okawa, H. *Inorg. Chem.* **1998**, *37*, 989. (g) Uozumi, S.; Furutachi, H.; Ohba, M.; Okawa, H.; Fenton, D. E.; Shindo, K.; Murata, S.; Kitko, D. J. *Inorg. Chem.* **1998**, *37*, 6281.
(7) (a) Arnold, M.; Brown, D. A.; Deeg, O.; Errington, W.; Haase, W.; Herlihy, K.; Kemp, T. J.; Nimir, H.; Werner, R. *Inorg. Chem.* **1998**, *37*, 2920. (b) Brown, D. A.; Cuffe, L. P.; Deeg, O.; Errington, W.; Fitzpatrick, N. J.; Glass, W. K.; Herlihy, K.; Kemp, T. J.; Nimir, H. *Chem. Commun.* **1998**, 2433.
(8) Yamaguchi, K.; Koshino, S.; Akagi, F.; Suzuki, M.; Uehara, A.; Suzuki, S. *J. Am. Chem. Soc.* **1997**, *119*, 5752.
(9) (a) Meyer, F.; Pritzkow, H. *Chem. Commun.* **1998**, 1555. (b) Meyer, F.; Kaifer, E.; Kircher, P.; Heinze, K.; Pritzkow, H. *Chem.—Eur. J.* **1999**, *5*, 1617.

10.1021/ic990137u CCC: $18.00
Published on Web 09/11/1999

Chart 1

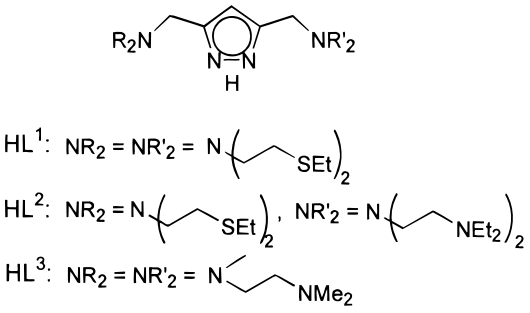

symmetric versus asymmetric geometry of the bimetallic core. The ability of the new complexes to promote the ethanolysis of urea is examined and is discussed in the light of their specific structural features.

Experimental Section

General Procedures and Methods. All manipulations were carried out under an atmosphere of dry nitrogen by employing standard Schlenk techniques. Solvents were dried according to established procedures. HL^1, HL^2, and HL^3 (Chart 1) were synthesized according to the reported methods;[10,11] all other chemicals were used as purchased. Microanalyses: Mikroanalytische Laboratorien des Organisch-Chemischen Instituts der Universität Heidelberg. IR spectra: Perkin-Elmer 983G; recorded as KBr pellets. FAB-MS spectra: Finnigan MAT 8230. UV/vis spectra: Perkin-Elmer Lambda 19. NMR spectra: Bruker AC 200 at 200.13 (^{1}H) and 50.32 (^{13}C) MHz, or Bruker DRX 300 at 300.13 MHz (^{1}H), or Bruker DRX 500 at 500.13 MHz (^{1}H). Magnetic measurements: Bruker magnet B-E 15 C8, field controller B-H 15, variable temperature unit ER4111VT, Sartorius microbalance M 25 D-S. Experimental susceptibility data were corrected for the underlying diamagnetism.

CAUTION! Although no problems were encountered in this work, transition metal perchlorate complexes are potentially explosive and should be handled with proper precautions.

Synthesis of 1. HL^1 (239 mg, 0.5 mmol) dissolved in methanol (15 mL) was deprotonated by means of addition of 1 equiv of KO^{t}Bu (56 mg). After this mixture was stirred for 10 min, a solution of $[Ni(H_2O)_6](ClO_4)_2$ (274 mg, 0.75 mmol) and $Ni(OAc)_2 \cdot 4H_2O$ (62 mg, 0.25 mmol) in methanol (15 mL) was added. The green reaction mixture was evaporated to dryness. Vapor diffusion of light petroleum into a solution of the resulting solid in acetone gave blue-green crystals of **1** (315 mg, 65%). IR (KBr, cm^{-1}): 1679 [s, ν(C=O)], 1572 [s, ν_{as}(COO)], 1416 [s, ν_s(COO)], 1094 [s, $\nu(ClO_4)$], 622 (s). MS (FAB+) [*m*/*z* (relative intensity)]: 753 (100) $[L^1Ni_2(OAc)(ClO_4)]^+$. Anal. Calcd for $C_{29}H_{56}Cl_2N_4Ni_2O_{12}S_4$: C, 35.93; H, 5.82; N, 5.78. Found: C, 35.22; H, 5.85; N, 5.74.

Synthesis of 2a. Urea (60 mg, 1.0 mmol) was added to a solution of **1**·$(ClO_4)_2$ (485 mg, 0.5 mmol) in ethanol (30 mL), resulting in a slight color change from green to blue-green. After stirring for 12 h at room temperature the reaction mixture was evaporated to dryness. Vapor diffusion of Et_2O into a solution of the crude product in methanol gave blue crystals of **2a** (321 mg, 66%). IR (KBr, cm^{-1}): 3417/3358 [s, ν(NH)], 1642 [s, ν(C=O)], 1618 (s), 1585 [s, ν_{as}(COO)], 1467 (s), 1415 [s, ν_s(COO)], 1114/1084 [s, $\nu(ClO_4)$], 625 (s). MS (FAB+) [*m*/*z* (relative intensity)]: 797 (100) $[L^1Ni_2(OAc)(ClO_4)(CONH_2)]^+$, 753 (92) $[L^1Ni_2(OAc)(ClO_4)]^+$. Anal. Calcd for $C_{25}H_{52}Cl_2N_8Ni_2O_{12}S_4$: C, 30.85; H, 5.39; N, 11.51. Found: C, 30.81; H, 5.43; N, 11.19.

Synthesis of 2b. This complex was prepared similarly to **2a** using *N*,*N*-dimethylurea. Yield: 355 mg (69%). IR (KBr, cm^{-1}): 3434−3200 [s, ν(NH)], 1637 [s, ν(C=O)], 1565 [s, ν_{as}(COO)], 1414 [s, ν_s(COO)], 1088 [s, $\nu(ClO_4)$], 623 (s). MS (FAB+) [*m*/*z* (relative intensity)]: 753 (92) $[L^1Ni_2(OAc)(ClO_4)]^+$. Anal. Calcd for $C_{29}H_{60}Cl_2N_8Ni_2O_{12}S_4$: C, 33.84; H, 5.87; N, 10.89. Found: C, 32.91; H, 6.06; N, 10.55.

Synthesis of 2c. This complex was prepared similarly to **2a** using benzylurea. Yield: 369 mg (64%). IR (KBr, cm^{-1}): 3411 [s, ν(NH)], 3311−3202 [s, ν(NH)], 1642 [s, ν(C=O)], 1593 [s, ν_{as}(COO)], 1545 (s), 1416 [s, ν_s(COO)], 1259 (s), 1088 [s, $\nu(ClO_4)$], 624 (s). MS (FAB+) [*m*/*z* (relative intensity)]: 753 (92) $[L^1Ni_2(OAc)(ClO_4)]^+$. Anal. Calcd for $C_{39}H_{64}Cl_2N_8Ni_2O_{12}S_4$: C, 40.61; H, 5.59; N, 9.71. Found: C, 40.15; H, 5.57; N, 9.59.

Synthesis of 3a. HL^2 (250 mg, 0.5 mmol) was dissolved in THF (15 mL) and deprotonated by means of addition of 1 equiv of KO^{t}Bu (56 mg). After this mixture was stirred for 10 min at room temperature, a solution of $[Ni(H_2O)_6](ClO_4)_2$ (274 mg, 0.75 mmol) and $Ni(OAc)_2 \cdot 4H_2O$ (62 mg, 0.25 mmol) in methanol (15 mL) was added. After treatment with urea (30 mg, 0.5 mmol) the formerly blue-green solution turned green. The reaction mixture was evaporated to dryness. Vapor diffusion of Et_2O into a solution of the product in methanol gave dark-green crystals of **3a** (267 mg, 57%). IR (KBr, cm^{-1}): 3435 [s, ν(NH)], 1654 [s, ν(C=O)], 1614 (s), 1583 [s, ν_{as}(COO)], 1408 (m), 1119/1106/1086 [s, $\nu(ClO_4)$]. MS (FAB+) [*m*/*z* (relative intensity)]: 775 (100), $[L^2Ni_2(OAc)(ClO_4)]^+$; 645 (30), $[LNi_2(OAc) - Et]^+$. Anal. Calcd for $C_{28}H_{58}Cl_2N_8Ni_2O_{11}S_2$: C, 35.96; H, 6.25; N, 11.98. Found: C, 35.89; H, 6.27; N, 11.92.

Synthesis of 3b. This complex was prepared similarly to **3a** using *N*,*N*-dimethylurea. Yield: 260 mg (54%). IR (KBr, cm^{-1}): 3401 [s, ν(NH)], 1648 [s, ν(C=O)], 1579 [s, ν_{as}(COO)], 1446 (s), 1415 [m, ν_s(COO)], 1108/1088 [s, $\nu(ClO_4)$], 622 (s). MS (FAB+) [*m*/*z* (relative intensity)]: 775 (100), $[L^2Ni_2(OAc)(ClO_4)]^+$; 645 (30), $[LNi_2(OAc) - Et]^+$. Anal. Calcd for $C_{30}H_{62}Cl_2N_8Ni_2O_{11}S_2$: C, 37.41; H, 6.49; N, 11.63. Found: C, 37.09; H, 6.48; N, 11.26.

Synthesis of 4. To a solution of HL^3 (0.16 g, 0.54 mmol) in EtOH (20 mL) were added 1 equiv of KO^{t}Bu (0.06 g, 0.54 mmol), 0.5 equiv of $Ni(OAc)_2 \cdot 4H_2O$ (0.07 g, 0.27 mmol), and 1.5 equiv of $[Ni(H_2O)_6](ClO_4)_2$ (0.29 g, 0.81 mmol). After being stirred for 30 min at room temperature, the reaction mixture was treated with an excess of *N*,*N*′-dimethylurea (1.0 g, 11.4 mmol), and stirring was continued for an additional 15 h. A small amount of precipitate was filtered off, and the now clear, slightly greenish-blue solution was evaporated to dryness. Layering a solution of the residue in MeOH with Et_2O afforded greenish-blue crystals of the product **4**·0.5MeOH (0.33 g, 66%). IR (KBr, cm^{-1}): 3399 [br, s, ν(OH)], 3244 (w), 1641 [s, ν(C=O)], 1560 [s, ν_{as}(COO)], 1454 (m), 1404 (m), 1095 [vs, $\nu(ClO_4)$], 810 (m), 624 (s). MS (FAB+) [*m*/*z* (relative intensity)]: 571 (100), $[L^3Ni_2(OAc)(ClO_4)]^+$; 472 (25), $[L^3Ni_2(OAc)]^+$. Anal. Calcd for $C_{25}H_{58}Cl_2N_{10}Ni_2O_{14}$: C, 32.96; H, 6.42; N, 15.37. Found: C, 32.60; H, 6.26; N, 15.14.

Synthesis of 5. HL^3 (0.21 g, 0.71 mmol) was dissolved in MeOH (20 mL) and treated with 2 equiv of $Ni(OAc)_2 \cdot 4H_2O$ (0.36 g, 1.42 mmol). After the resulting greenish-blue solution was stirred for 30 min at room temperature, $NaBPh_4$ (0.26 g, 0.76 mmol) was added and stirring continued for an additional 2 h. All volatile material was then evaporated under reduced pressure and the residue taken up in acetone and layered with light petroleum to gradually afford greenish-blue crystals of **5**·H_2O·2acetone (0.31 g, 41%). IR (KBr, cm^{-1}): 3419 [br, m, ν(OH)], 3260 (br, m), 1702 [m, ν(C=O), acetone], 1584 [s, ν_{as}(COO)], 1548 [s, ν_{as}(COO)], 1449 (s), 1420 (m), 1405 (m), 743 (m), 732 (m), 710 (m), 700 (m), 675 (m), 612 (m). MS (FAB+) [*m*/*z* (relative intensity)]: 611 (40), $[L^3Ni_2(OAc)_3Na]^+$; 529 (100), $[L^3Ni_2(OAc)_2]^+$; 470 (17), $[L^3Ni_2(OAc)]^+$. Anal. Calcd for $C_{21}H_{40}N_6Ni_2O_6 \cdot C_{24}H_{20}BNa \cdot H_2O \cdot 2C_3H_6O$: C, 57.44; H, 6.99; N, 7.88. Found: C, 57.57; H, 6.93; N, 8.40.

Ethanolysis of Urea. An ethanol solution (30 mL) containing the respective complex (0.05 mmol, i.e., 1.7 mM in solution) or a mixture of the free ligand and 2 equiv of $[Ni(H_2O)_6](ClO_4)_2$ (compare Table 9), 30 equiv of urea, and inert 1,3,5-trimethoxybenzene (0.10 mmol, i.e., 3.3 mM in solution) as an internal standard was stirred under reflux for 6 days. After removal of the solvent under reduced pressure the reaction mixture was extracted with 50 mL of CH_2Cl_2 and the organic phase again evaporated to dryness. The residue was taken up in dmso-d_6 and analyzed by ^{1}H NMR spectroscopy. The amount of product

(10) Konrad, M.; Meyer, F.; Heinze, K.; Zsolnai, L. *J. Chem. Soc., Dalton Trans.* **1998**, 199.
(11) Meyer, F.; Ruschewitz, U.; Schober, P.; Antelmann, B.; Zsolnai, L. *J. Chem. Soc., Dalton Trans.* **1998**, 1181.

Table 1. Crystal Data and Refinement Details for Complexes **1**, **2c**, **3a**, **4**, and **5**

	1	**2c**	**3a**	**4**·0.5MeOH	**5**·H_2O·2acetone
formula	$C_{29}H_{52}Cl_2N_4Ni_2O_{12}S_4$	$C_{39}H_{64}Cl_2N_8Ni_2O_{12}S_4$	$C_{28}H_{58}Cl_2N_8Ni_2O_{11}S_2$	$C_{25}H_{52}Cl_2N_{10}Ni_2O_{14}$·0.5MeOH	$C_{39}H_{55}BN_6NaNi_2O_6$·2 acetone·$H_2O$
M_r	969.32	1153.52	935.26	920.60	989.26
cryst size (mm)	0.20 × 0.20 × 0.30	0.10 × 0.10 × 0.20	0.10 × 0.10 × 0.10	0.25 × 0.25 × 0.30	0.20 × 0.20 × 0.20
crystal syst	monoclinic	triclinic	monoclinic	monoclinic	monoclinic
space group	*C*2/*c*	$P\bar{1}$	$P2_1/c$	$P2_1/c$	$P2_1/n$
a (Å)	25.027(4)	10.764(2)	13.932(3)	18.538(4)	15.129(3)
b (Å)	11.593(2)	11.242(2)	18.748(4)	12.072(2)	9.900(2)
c (Å)	14.556(2)	23.776(5)	15.517(3)	19.971(4)	37.062(7)
α (deg)	90	93.19(3)	90	90	90
β (deg)	95.82(1)	95.28(3)	91.07(3)	98.54(3)	104.14(1)
γ (deg)	90	113.15(3)	90	90	90
V (Å^3)	4201(1)	2621(1)	4052(2)	4420(2)	5446(2)
ρ_{calcd} (g cm^{-3})	1.499	1.462	1.533	1.383	1.298
Z	4	2	4	4	4
F(000) (e)	1948	1208	1968	1930	2256
T (K)	200	200	200	200	200
μ(Mo Kα) (mm^{-1})	0.710 73	0.710 73	0.710 73	0.710 73	0.710 73
scan mode	*ω*	*ω*	*ω*	*ω*	*ω*
hkl range	±30, ±14, ±17	±13, ±13, ±29	±17, −22 to 23, ±19	±25, ±16, −27 to 24	−4 to 18, ±11, ±44
2*θ* range (deg)	3.3−51.9	3.5−52.0	2.9−52.4	4.0−59.1	2.2−51.0
measured reflns	30 409	26 146	54 980	38 858	10 492
unique reflns	4073	9346	8001	12333	10090
observed reflns $I > 2\sigma(I)$	2640	6033	3282	7594	4658
refined params	273	627	535	547	602
residual electron density (e Å^{-3})	1.58/−1.14	2.26/−0.51	0.52/−0.45	1.45/−0.58	0.61/−0.65
R1	0.078	0.061	0.058	0.058	0.098
wR2	0.241	0.196	0.162	0.198	0.273
goodness of fit	1.204	1.051	0.854	1.036	1.049

formation was estimated by integration of the signals for ethyl carbamate (in particular the quadruplet at $\delta = 3.92$ ppm) and for the internal standard.

X-ray Crystallography. The measurements were carried out on a Nonius Kappa CCD diffractometer (complexes **1**, **2c**, **3a**, **4**) or a Siemens P4 four-circle diffractometer (complex **5**) using graphite-monochromated Mo Kα radiation. For **5** the intensities of three check reflections (measured every 100 reflections) remained constant throughout the data collection, thus indicating crystal and electronic stability. All calculations were performed using the SHELXT PLUS software package. Structures were solved by direct methods with the SHELXS-97 program and refined with the SHELXL-97 program.[12] For **5** an absorption correction (ψ scan, $\Delta\psi = 10°$) was applied to the data. Atomic coordinates and thermal parameters of the non-hydrogen atoms were refined in fully or partially anisotropic models by full-matrix least-squares calculation based on F^2. In general the hydrogen atoms were placed at calculated positions and allowed to ride on the atoms they are attached to. In the case of **2c** and **3a** the N-bound hydrogen atoms of the urea ligands could be located in the difference Fourier map and refined. Due to the poor quality of the crystal, the structure analysis of **1** and **5** could only be refined to final (poor) agreement values of R1 = 0.078 and 0.098, respectively. Table 1 compiles the data for the structure determinations.

Results and Discussion

Synthesis and Characterization. The pyrazolate ligands L^1, L^2, and L^3 bearing multiple donor sites within chelating side arms attached to the heterocycle are employed in the present work. L^1 has previously been shown to favor 6-fold coordination in its dinickel(II) complexes by accommodating additional exo ligands at each metal center.[10] With the aim of establishing a versatile starting material for the synthesis of the sought-after urea adducts, the complex $[L^1Ni_2(\mu\text{-OAc})(\text{acetone})_2]^{2+}$ was prepared and obtained in crystalline form as its perchlorate salt **1**. It crystallizes in the monoclinic space group *C*2/*c* with four molecular entities in the unit cell.

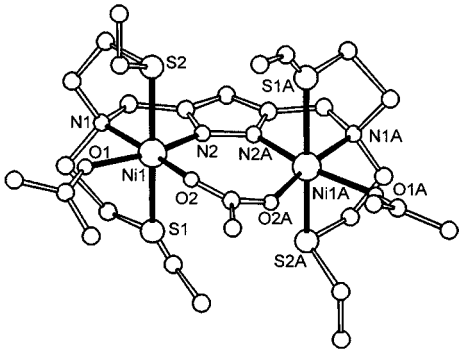

Figure 1. View of the molecular structure of the cation of **1**. In the interest of clarity most of the hydrogen atoms have been omitted.

The X-ray structural analysis (Figure 1; selected atom distances and bond angles are listed in Table 2) confirms the presence of two nickel ions in distorted OC-6 environments spanned by the pyrazolate and a secondary acetate bridge. The Ni···Ni distance (4.161 Å) is slightly elongated compared to a related Cl-bridged complex (3.823 Å)[10] due to the strain imposed by the comparatively larger three-atom acetate bridge. This is also reflected in a considerable tilting of the acetate moiety with respect to the plane defined by the pyrazolate (17.4°).

Six-coordination of the metal centers in **1** is also retained in solution as evidenced by the UV/vis absorption spectrum (Table 3). It displays three ligand field transitions at 1029 (ν_1), 607 (ν_2), and 388 (ν_3) nm assigned to spin-allowed transitions from $^3A_{2g}$ to $^3T_{2g}$, $^3T_{1g}$(F), and $^3T_{1g}$(P), respectively, in accord with

(12) Sheldrick, G. M. *SHELXL-97, Program for Crystal Structure Refinement*; Universität Göttingen: Göttingen, 1997. Sheldrick, G. M. *SHELXS-97, Program for Crystal Structure Solution*; Universität Göttingen, Göttingen, 1997.

Table 2. Selected Atom Distances (Å) and Angles (deg) for **1**

Ni1−N2	2.002(5)	Ni1−S2	2.456(2)
Ni1−O2	2.015(4)	Ni1−S1	2.531(4)
Ni1−O1	2.167(5)	Ni1···Ni1A	4.161
Ni1−N1	2.168(5)		
N2−Ni1−O2	106.2(2)	O1−Ni1−S2	87.1(2)
N2−Ni1−O1	166.7(2)	N1−Ni1−S2	84.6(2)
O2−Ni1−O1	87.0(2)	N2−Ni1−S1	79.1(2)
N2−Ni1−N1	80.6(2)	O2−Ni1−S1	99.3(2)
O2−Ni1−N1	172.4(2)	O1−Ni1−S1	100.5(2)
O1−Ni1−N1	86.1(2)	N1−Ni1−S1	85.1(2)
N2−Ni1−S2	91.1(2)	S2−Ni1−S1	166.8(2)
O2−Ni1−S2	91.9(2)		

Table 3. UV/Vis Data of the Complexes. in cm^{-1} (ϵ in M^{-1} cm^{-1})

1	25 800 (170), 16 480 (55), 9700 (65)
2a	25 580 (85), 16 420 (30), 9700 (55)
2b	25 710 (115), 16 420 (30), 9550 (65)
2c	25 520 (105), 16 390 (30), 9500 (60)
3a	25 390 (175), 16 080 (60), 8800 (60)
3b	25 300 (155), 15 990 (50), 8500 (60)

Chart 2

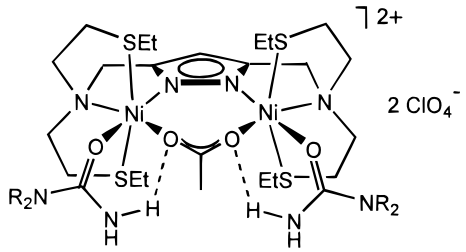

NR_2 = NH_2 (**2a**), NMe_2 (**2b**), $NH(CH_2Ph)$ (**2c**)

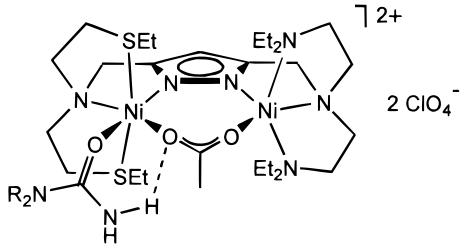

NR_2 = NH_2 (**3a**), NMe_2 (**3b**)

d^8 ions in near octahedral coordination spheres.[13] The value $\Delta_{oct} \approx 9700$ cm^{-1} can be deduced from the ν_1 band, and a calculated Racah parameter $B \approx 940$ cm^{-1} results from consideration of an octahedral strong-field coupling scheme. Taking $15B = 15\,615$ cm^{-1} for the gaseous ion $Ni^{2+}(^3P)$,[14] this leads to a reasonable nephelauxetic ratio β of 0.90.

Treatment of a solution of **1** in ethanol with urea or its derivatives (Chart 2) causes a slight change in color from green to blue-green, and the urea adducts **2a**−**c** can be isolated in crystalline form after appropriate workup. Owing to the similarity of their spectroscopic properties (vide supra), a similar molecular structure for all three compounds is suggested, and the benzyl derivative **2c** was taken as a representative example for crystallographic analysis. Its perchlorate salt crystallizes in the triclinic space group $P\bar{1}$. The structure of the cation is depicted in Figure 2; selected atom distances and bond angles are given in Table 4.

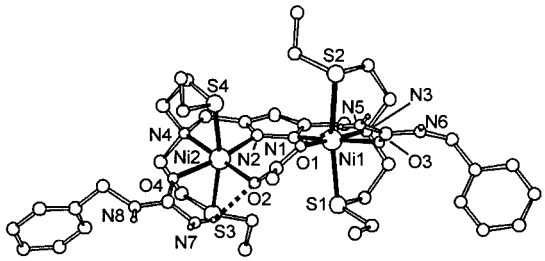

Figure 2. View of the molecular structure of the cation of **2c**. In the interest of clarity most of the hydrogen atoms have been omitted.

Table 4. Selected Atom Distances (Å) and Angles (deg) for **2c**

Ni1−N1	2.003(5)	Ni2−O2	2.086(4)
Ni1−O1	2.036(4)	Ni2−O4	2.093(4)
Ni1−O3	2.102(4)	Ni2−N4	2.140(4)
Ni1−N3	2.143(5)	Ni2−S4	2.423(2)
Ni1−S1	2.440(2)	Ni2−S3	2.442(2)
Ni1−S2	2.453(2)	Ni1···Ni2	4.196
Ni2−N2	1.999(4)		
N1−Ni1−O1	101.5(2)	N2−Ni2−O2	98.4(2)
N1−Ni1−O3	167.5(2)	N2−Ni2−O4	168.0(2)
O1−Ni1−O3	91.0(2)	O2−Ni2−O4	93.7(2)
N1−Ni1−N3	81.0(2)	N2−Ni2−N4	81.1(2)
O1−Ni1−N3	176.2(2)	O2−Ni2−N4	179.5(2)
O3−Ni1−N3	86.5(2)	O4−Ni2−N4	86.9(2)
N1−Ni1−S1	88.7(2)	N2−Ni2−S4	90.7(2)
O1−Ni1−S1	95.5(2)	O2−Ni2−S4	92.6(2)
O3−Ni1−S1	89.4(2)	O4−Ni2−S4	88.9(2)
N3−Ni1−S1	87.4(2)	N4−Ni2−S4	87.4(2)
N1−Ni1−S2	95.2(2)	N2−Ni2−S3	96.2(2)
O1−Ni1−S2	92.1(2)	O2−Ni2−S3	94.2(2)
O3−Ni1−S2	85.1(2)	O4−Ni2−S3	82.7(2)
N3−Ni1−S2	84.8(2)	N4−Ni2−S3	85.9(2)
S1−Ni1−S2	170.7(1)	S4−Ni2−S3	169.5(1)

As anticipated, the basic dinuclear framework of **1** has been preserved in **2c**, while the formerly bound acetone ligands have now been replaced by O-coordinated urea molecules. However, whereas the Ni···Ni distances in **1** and **2c** differ only slightly (4.161 vs 4.196 Å), the exchange of acetone by urea induces geometric changes of the dinuclear core that are more severe than expected. The equatorial N_2O_2 planes of the nickel ligation sphere in **2c** are considerably tilted against each other (27.4°) and also with respect to the pyrazolate heterocycle [15.9° (Ni1) and 13.9° (Ni2)], which goes along with a distinct tilting of the acetate moiety with respect to the pyrazolate plane (45.2°) and causes the nickel ions to lie 0.54 Å (Ni1) and 0.44 Å (Ni2) above and below the latter plane, respectively. This particular distortion appears to be constrained mainly by hydrogen bridges between the amino groups of the coordinated urea molecules and the O atoms of the acetate bridge [d(N5···O1) = 2.794 Å; d(N7···O2) = 2.813 Å], which presumably contribute to the fixation of the potential substrate at the dinuclear core. Further weak hydrogen bonds between the other NH functions of the bound urea and the oxygen atoms of perchlorate counteranions are present in the crystal lattice [d(N···O) = 2.93−3.02 Å]. The Ni−O(urea) distances of 2.102(4) and 2.093(4) Å are typical for this type of linkage.[6b]

The IR spectra of **2a**−**c** contain several features in the range 1650−1540 cm^{-1} arising from ν(C═O) of bound urea and ν_{as}(COO) of the bridging acetate. Among these, intense bands at 1642 (**2a**), 1637 (**2b**), and 1642 cm^{-1} (**2c**) are assigned to the carbonyl stretching mode of the respective urea and corroborate the presence of its O-bonded linkage isomers, in which the

(13) Nicholls, D. In *Comprehensive Inorganic Chemistry*; Bailar, J. C., Emeleus, H. J., Nyholm, R., Trotman-Dickenson, A. F., Eds.; Pergamon: Oxford, 1973; Vol. 3, p 1152 ff.

(14) Huheey, J.; Keiter, E.; Keiter, R. *Anorganische Chemie*, 2nd ed.; Walter de Gruyter: Berlin, 1995; p 517.

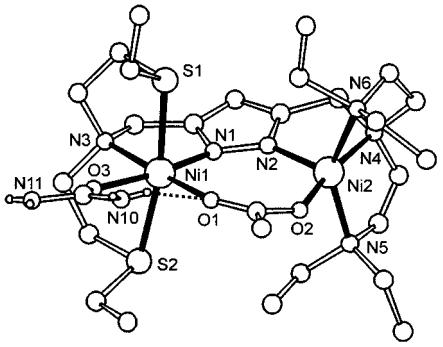

Figure 3. View of the molecular structure of the cation of **3a**. In the interest of clarity most of the hydrogen atoms have been omitted.

Table 5. Selected Atom Distances (Å) and Angles (deg) for **3a**

Ni1−N1	2.032(5)	Ni2−N2	1.975(4)
Ni1−O1	2.060(4)	Ni2−O2	1.973(4)
Ni1−O3	2.063(4)	Ni2−N4	2.098(5)
Ni1−N3	2.138(5)	Ni2−N5	2.123(5)
Ni1−S1	2.466(2)	Ni2−N6	2.139(6)
Ni1−S2	2.504(2)	Ni1···Ni2	4.221
N1−Ni1−O1	100.6(2)	N3−Ni1−S2	84.4(2)
N1−Ni1−O3	168.0(2)	S1−Ni1−S2	169.6(2)
O1−Ni1−O3	91.4(2)	N2−Ni2−O2	108.4(2)
N1−Ni1−N3	81.1(2)	N2−Ni2−N4	82.8(2)
O1−Ni1−N3	176.2(2)	O2−Ni2−N4	168.4(2)
O3−Ni1−N3	86.8(2)	N2−Ni2−N5	102.0(2)
N1−Ni1−S1	87.7(2)	O2−Ni2−N5	94.8(2)
O1−Ni1−S1	91.1(2)	N4−Ni2−N5	85.6(2)
O3−Ni1−S1	91.3(2)	N2−Ni2−N6	108.8(3)
N3−Ni1−S1	85.6(2)	O2−Ni2−N6	90.2(2)
N1−Ni1−S2	93.7(2)	N4−Ni2−N6	83.1(2)
O1−Ni1−S2	98.8(2)	N5−Ni2−N6	145.5(3)
O3−Ni1−S2	85.2(2)		

C═O bond is weakened and its stretching frequency shifted to wavelengths <1700 cm^{-1}.[15] The facile loss of these urea ligands is inferred from the mass spectra showing an intense signal at $m/z = 753$ corresponding to $[L^1Ni_2(OAc)(ClO_4)]^+$ in all cases **2a**−**c**. The optical absorption spectra of **2a**−**c** (Table 3) and the ligand field characteristics deduced from these are similar to those of **1**, with Δ_{oct} in the range 9500−9700 cm^{-1} and calculated Racah parameters B of 910−950 cm^{-1}.

The synthesis of related unsymmetrical systems **3a**,**b** that feature coordination of urea at only one metal center was achieved starting from the ligand L^2, which has previously been proven to afford geometrically asymmetric dinickel(II) complexes with a {5/6} coordination number set.[10] The molecular structure of **3a** was elucidated by X-ray crystallography and is depicted in Figure 3; selected atom distances and bond angles are listed in Table 5.

In accord with previous findings, the "nitrogen-only" side arm restricts its respective nickel center to five-coordination with a geometry intermediate between SPY-5 and TB-5 based on the τ criterion [τ(Ni2) = 0.38].[16] On the other hand the N_2S_2 compartment of L^2 accommodates its nickel ion in a manner similar to the situation found in **2c**, i.e., it allows for additional exo binding of a urea substrate molecule [d(N1−O3)] = 2.063(4) Å]. The latter is again supported by hydrogen bridging between a suitably positioned urea amino group and an oxygen atom of the acetate bridge [d(N10···O1) = 2.899 Å]. The tilting of the three-atom acetate bridge with respect to the pyrazolate amounts to 24.1° in **3a**, bringing about a Ni···Ni distance of 4.221 Å and forcing the Ni1 atom to lie 0.520 Å out of the plane of the heterocycle. These considerable deviations from coplanarity of the N_2O_2 equatorial Ni1 coordination plane and the pyrazolate heterocycle as well as the obvious puckering of the overall bimetallic core of **3a** are in contrast to the much less distorted structure of a related asymmetric dinickel(II) complex featuring a smaller one-atom Cl secondary bridge.[10]

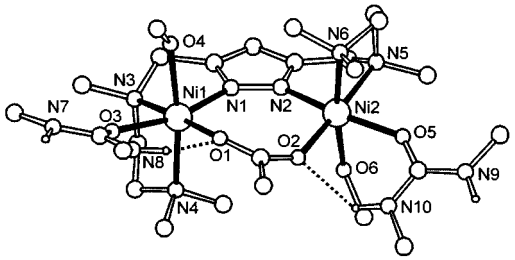

Figure 4. View of the molecular structure of the cation of **4**. In the interest of clarity most of the hydrogen atoms have been omitted.

Table 6. Selected Atom Distances (Å) and Angles (deg) for **4**

Ni1−N1	2.045(3)	Ni2−O2	2.056(2)
Ni1−O1	2.057(2)	Ni2−O5	2.056(2)
Ni1−O3	2.097(2)	Ni2−N6	2.170(3)
Ni1−N4	2.137(3)	Ni2−O6	2.178(3)
Ni1−O4	2.145(3)	Ni2−N5	2.182(3)
Ni1−N3	2.189(3)	Ni1···Ni2	4.316
Ni2−N2	2.023(3)		
N1−Ni1−O1	100.8(1)	N2−Ni2−O2	99.8(1)
N1−Ni1−O3	163.8(2)	N2−Ni2−O5	166.3(1)
O1−Ni1−O3	92.7(1)	O2−Ni2−O5	92.2(1)
N1−Ni1−N4	100.1(2)	N2−Ni2−N6	98.6(2)
O1−Ni1−N4	92.3(2)	O2−Ni2−N6	93.3(2)
O3−Ni1−N4	88.3(2)	O5−Ni2−N6	87.4(2)
N1−Ni1−O4	85.8(2)	N2−Ni2−O6	85.3(2)
O1−Ni1−O4	91.3(2)	O2−Ni2−O6	93.0(2)
O3−Ni1−O4	84.9(2)	O5−Ni2−O6	87.4(2)
N4−Ni1−O4	172.5(2)	N6−Ni2−O6	172.0(2)
N1−Ni1−N3	79.4(2)	N2−Ni2−N5	79.6(2)
O1−Ni1−N3	176.9(2)	O2−Ni2−N5	177.3(2)
O3−Ni1−N3	87.8(2)	O5−Ni2−N5	88.8(2)
N4−Ni1−N3	84.6(2)	N6−Ni2−N5	84.2(2)
O4−Ni1−N3	91.9(2)	O6−Ni2−N5	89.6(2)

Strong IR absorptions between 1655 and 1575 cm^{-1} for **3a**,**b** are again characteristic for ν(C═O) of bound urea as well as ν_{as}(COO) of the bridging acetate, and the occurrence of ν(C═O) at 1652 (**3a**) and 1648 cm^{-1} (**3b**) is indicative of urea binding through its oxygen atom in these adducts. A major signal at $m/z = 775$ corresponding to $[L^2Ni_2(OAc)(ClO_4)]^+$ in the mass spectra underlines the easy loss of such urea ligands.

In a further variation of the bimetallic framework, the dinucleating ligand L^3 possessing fewer donor sites within its chelating side arms was employed in order to provide potentially accessible coordination sites at the resulting dinickel(II) systems.[11] The molecular structure of the complex $[L^3Ni_2(\mu\text{-OAc})(N,N'\text{-dimethylurea})_2(MeOH)_2]^{2+}$, which could be obtained in crystalline form as its perchlorate salt **4** from MeOH/Et_2O, is shown in Figure 4; selected atom distances and bond angles are given in Table 6.

The metal centers in **4** are found to be six-coordinate, each being nested in a *fac*-tridentate coordination compartment of L^3 and bound to the O atoms of the secondary acetate bridge, a *N*,*N*′-dimethylurea ligand, and a methanol solvent molecule.

(15) Maslak, P.; Sczepanski, J. J.; Parvez, M. *J. Am. Chem. Soc.* **1991**, *113*, 1062.

(16) Addison, A. W.; Rao, T. N.; Reedijk, J.; van Rijn, J.; Verschoor, G. C. *J. Chem. Soc., Dalton Trans.* **1984**, 1349. $\tau = (\beta - \alpha)/60$, where α and β represent two basal angles with $\beta > \alpha$. A perfect TB-5 structure is associated with $\tau = 1$, while $\tau = 0$ is expected for ideal SPY-5 geometry.

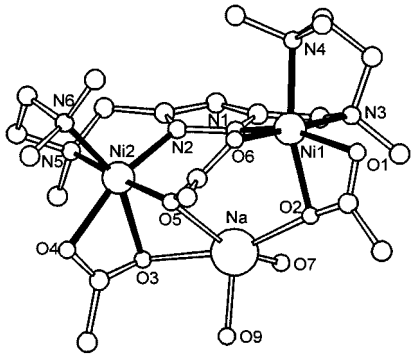

Figure 5. View of the molecular structure of the cation of **5**. In the interest of clarity the hydrogen atoms have been omitted.

The coordination spheres of the nickel(II) centers appear to be axially elongated with rather long bonds Ni1−O4, Ni1−N4 and Ni2−O6, Ni2−N6 (2.13−2.18 Å), respectively. Permitted by a slightly longer and thereby more relaxed Ni···Ni separation of 4.316 Å, the tilting of the acetate with respect to the pyrazolate is less distinct in **4** than in the aforementioned cases **2c** and **3a**, and the nickel ions are now located roughly within the plane defined by the heterocycle (distance 0.066/0.023 Å). The *N*,*N*′-dimethylurea entities adopt the expected all-trans configuration and again form hydrogen bridges to the O atoms of the acetate bridge [d(N8···O1) = 2.838 Å; d(N10···O2) = 2.883 Å]. The coordinated methanol molecules are located trans to each other on opposite sides of the bimetallic framework, resulting in an approximate (noncrystallographic) C_2 symmetry of the complex. Consideration of the overall charges within the unit cell confirms that the methanol ligands are electrostatically neutral and thus protonated. These OH protons and the remaining NH moieties of the urea are involved in extensive hydrogen bonding to O atoms of the perchlorate counteranions and to an additional methanol solvent molecule included in the crystal lattice.

Intense IR absorptions at 1641 and 1560 cm^{-1} for **4** are assigned to the carbonyl stretching frequency of the O-bound urea ligands and ν_{as}(COO) of the bridging carboxylate, respectively. As expected, the mass spectrum of **4** displays a dominant signal at m/z = 571 corresponding to the fragment ion [L^3Ni_2(OAc)(ClO_4)]$^+$, again indicating the easy detachment of both the urea and methanol ligands from the dinuclear core.

When the reaction of L^3 with 2 equiv of nickel(II) is carried out in the presence of an excess of acetate, after addition of $NaBPh_4$ a different complex **5** is obtained, which can be crystallized from wet acetone/light petroleum. Its IR spectrum reveals the presence of at least two types of carboxylates [bands at 1584 and 1548 cm^{-1} in the ν_{as}(COO) region and at 1449, 1420, and 1405 cm^{-1} in the ν_s(COO) region], which is finally confirmed by an X-ray diffraction analysis of green crystals of **5**. The incorporation of 1 equiv of Na^+ within the complex is evidenced by the FAB mass spectrum showing dominant signals for both [$L^3Ni_2(OAc)_2$]$^+$ and the molecular ion [$L^3Ni_2(OAc)_3$Na]$^+$. The result of the X-ray crystallographic determination is depicted in Figure 5 along with selected atom distances and bond angles that are given in Table 7.

The two nickel ions each reside in a *fac*-tridentate coordination pocket of the primary ligand core and are spanned by both the pyrazolate and a symmetrically bridging bidentate acetate. An additional acetate is bound to each of the nickel centers in a symmetrically chelating mode [d(Ni−O) = 2.11−2.23 Å], thereby completing a distorted OC-6 coordination sphere of the metal ions. These latter two chelating acetates are located cis to each other with respect to the bimetallic framework, and a sodium ion is situated in close proximity on this particular side of the complex to favorably interact with one O atom of each of the carboxylates [d(Na−O2) = 2.260(7) Å, d(Na−O3) = 2.347(7) Å, d(Na−O5) = 2.501(7) Å]. Consequently, the bridging acetate moiety is again severely tilted with respect to the plane of the pyrazolate (46.6°), and the nickel atoms are thus enforced to lie 0.492 Å (Ni1) and 0.820 Å (Ni2) above and below the latter plane. The sodium ion is found in an overall five-coordination of O donors, where the environment is built of the three carboxylate O atoms, a water molecule [d(Na−O9) = 2.326(7) Å], and an acetone solvent molecule [d(Na−O7) = 2.298(7) Å]. Its coordination geometry can be viewed as predominantly SPY-5 (based on the τ criterion: $\tau = 0.10$)[16] with the water ligand located in the apical position. The protons of this water molecule are themselves involved in hydrogen bonding to two additional acetone molecules included in the crystal lattice [d(O9···O7#) = 2.821 Å, d(O9···O8) = 2.847 Å; O7# belongs to a symmetry-related neighboring acetone molecule].

Table 7. Selected Atom Distances (Å) and Angles (deg) for **5**

Ni1−N1	2.020(8)	Ni2−N5	2.153(9)
Ni1−O6	2.065(6)	Ni2−O3	2.221(6)
Ni1−N4	2.110(7)	Na−O2	2.260(7)
Ni1−O2	2.124(6)	Na−O7#1	2.298(7)
Ni1−N3	2.173(7)	Na−O9#2	2.326(7)
Ni1−O1	2.180(6)	Na−O3	2.347(7)
Ni2−N2	1.992(7)	Na−O5	2.501(7)
Ni2−N6	2.096(9)	Ni1···Ni2	4.291
Ni2−O5	2.108(7)	Ni1···Na	3.312
Ni2−O4	2.116(6)	Ni2···Na	3.253
N1−Ni1−O6	100.5(3)	O5−Ni2−O4	90.0(3)
N1−Ni1−N4	97.3(3)	N2−Ni2−N5	81.5(3)
O6−Ni1−N4	93.5(3)	N6−Ni2−N5	84.6(5)
N1−Ni1−O2	101.7(3)	O5−Ni2−N5	175.2(3)
O6−Ni1−O2	86.9(2)	O4−Ni2−N5	93.6(3)
N4−Ni1−O2	160.6(3)	N2−Ni2−O3	98.3(3)
N1−Ni1−N3	82.3(3)	N6−Ni2−O3	154.8(3)
O6−Ni1−N3	177.0(3)	O5−Ni2−O3	85.8(2)
N4−Ni1−N3	84.9(3)	O4−Ni2−O3	60.8(2)
O2−Ni1−N3	93.8(3)	N5−Ni2−O3	93.2(4)
N1−Ni1−O1	161.5(3)	O2−Na−O7#1	93.6(2)
O6−Ni1−O1	86.9(3)	O2−Na−O9#2	98.8(3)
N4−Ni1−O1	99.1(3)	O7#1-Na−O9#2	112.9(3)
O2−Ni1−O1	61.4(2)	O2−Na−O3	160.3(3)
N3−Ni1−O1	90.8(3)	O7#1-Na−O3	95.5(2)
N2−Ni2−N6	106.2(3)	O9#2-Na−O3	93.7(3)
N2−Ni2−O5	94.0(3)	O2−Na−O5	89.6(2)
N6−Ni2−O5	98.3(4)	O7#1-Na−O5	154.3(3)
N2−Ni2−O4	158.4(3)	O9#2-Na−O5	91.7(2)
N6−Ni2−O4	94.2(3)	O3−Na−O5	74.8(2)

These overall structural findings for the new complexes clearly demonstrate the ability of carboxylate moieties that bridge two nickel(II) ions to further contribute to the binding of either additional metal ions (as in **5**) or potential substrate molecules (via H-bonding as in **2c**, **3a**, **4**), and they thus underline the versatility in coordination potential that contributes to the ubiquitous occurrence of such carboxylates in bioinorganic systems.[17]

Magnetic Properties. The magnetic properties of powdered samples of **1**, **2a**, **3a**, and **4** in the solid state have been studied at 10 kG, over the temperature range 4.8−295 K. The data obtained for the molar susceptibility and the effective magnetic moment are plotted in Figure 6.

(17) (a) Kaim, W.; Schwederski, B. *Bioanorganische Chemie*; B. G. Teubner: Stuttgart, 1991. (b) Rardin, R. L.; Tolman, W. B.; Lippard, S. J. *New J. Chem.* **1991**, *15*, 417.

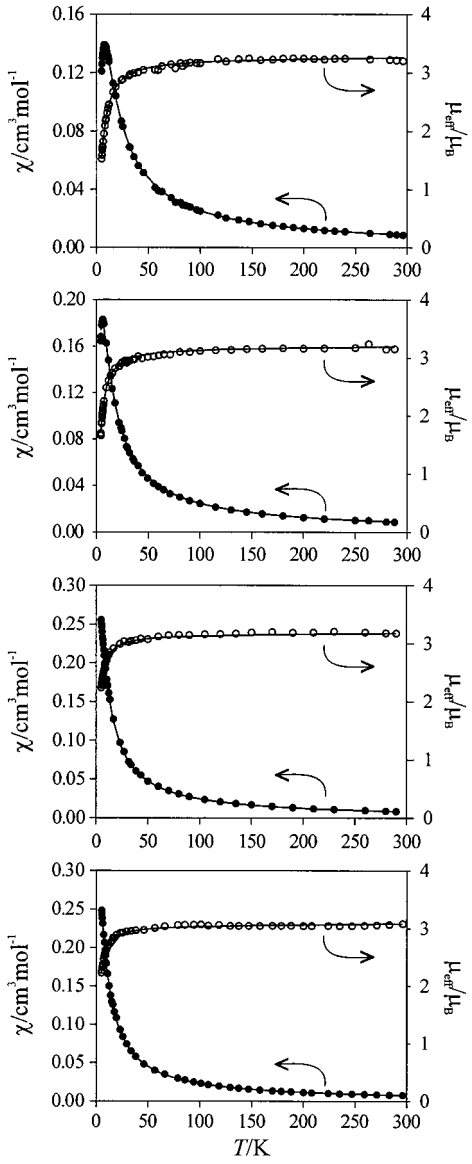

Figure 6. Temperature dependence of the molar magnetic susceptibility (solid circles) and magnetic moment (open circles) per nickel atom for **1** (top), **2a** (second from top), **3a** (third from top) and **4** (bottom). The solid lines represent the calculated curve fits.

The magnetic moment per nickel ion gradually decreases from 3.20 μ_B (**1**) and 3.15 μ_B (**2a**) at around 295 K to 1.52 μ_B (**1**) and 1.66 μ_B (**2a**) at 4.8 K, while the susceptibility curve exhibits a sharp maximum at 7.9 K (**1**) and 5.8 K (**2a**), this behavior being indicative of antiferromagnetic coupling between two nickel(II) centers. Modeling the experimental data by the standard expression for the isotropic spin-Hamiltonian $H = -2J\mathbf{S}_1\cdot\mathbf{S}_2$ (with $S_1 = S_2 = 1$) including a molar fraction p of uncoupled paramagnetic impurity (eq 1)[18,19] yields $J = -2.6 \pm 0.1$ cm^{-1}, $g = 2.30$ for **1** and $J = -1.9 \pm 0.1$ cm^{-1}, $g = 2.25$ for **2a** (Table 8).

$$\chi = \chi_{dim}(1 - p) + 2\chi_{mono}p + 2N_\alpha \qquad (1)$$

In principle, powder measurements are not ideally suited for a thorough analysis of $S = 1$ dinuclear systems; however, the intradimer exchange term J often is the dominant term in the spin Hamiltonian[20] and proved to be relatively insensitive to the magnitude of a zero-field splitting term D for the individual nickel ions. Accordingly, the neglect of both a parameter D as well as interdimer interactions $z'J'$ results in good quality fits in the present case (Figure 6, Table 8). The g values are reasonable, falling near the range 2.0−2.4 for octahedral nickel(II).[21]

Table 8. Magnetic Data for the Complexes

	g	J/cm^{-1}	p	R	d(Ni···Ni)
1	2.30	-2.6 ± 0.1	<0.01	1.3×10^{-4}	4.161
2a	2.25	-1.9 ± 0.1	<0.01	4.1×10^{-4}	4.196
3a	2.23	-1.3 ± 0.1		9.3×10^{-5}	4.221
4	2.16	-1.2 ± 0.1		4.9×10^{-5}	4.316

Antiferromagnetic exchange ranging from weak to moderate is quite frequently observed in pyrazolato[22,23] and carboxylato[6b] bridged dinickel(II) systems, and we assume that both available pathways contribute to the magnetic coupling in **1** and **2a**. Magnetostructural relationships for dinuclear Ni(II) systems are not yet very elaborated and are generally hampered by simultaneous changes of several structural parameters for the variety of complexes studied previously. Taking for granted the structural similarity of **2a**−**c**, the Ni···Ni separation is large and quite similar in both **1** and **2a**, while the most obvious structural difference between the two bimetallic cores is the more distinct tilt of the bridging acetate moiety with respect to the pyrazolate plane and the resulting displacement of the metal centers out of this latter plane in the urea adduct **2a**. This situation should go along with a less efficient orbital overlap between the nickel(II) ions and the bridging entities and might thus account for the slight reduction of the superexchange when going from **1** to **2a**. It has to be noted, though, that the small difference in J (0.7 cm^{-1}) as well as the limited number of only two systems taken into consideration precludes any conclusive magnetostructural correlations.

For **3a** and **4** the magnetic moment per nickel ion also decreases gradually when the temperature is lowered (Figure 6), but the antiferromagnetic coupling is less pronounced since no characteristic maximum in the $\chi(T)$ curve is reached within the temperature range studied (it should again be emphasized that zero-field splitting effects may well contribute to the observed magnetic behavior but are not accounted for in the

(18) (a) O'Connor, C. J. *Prog. Inorg. Chem.* **1982**, *29*, 203. (b) Kahn, O. *Molecular Magnetism*; VCH: Weinheim, 1993.

(19) N_α refers to the temperature-independent paramagnetism [100×10^{-6} cm^3/mol per nickel(II) ion[18b]]; all other parameters have their usual meaning.

$$\chi_{dim} = (Ng^2\mu_B{}^2/kT)\cdot[2\exp(2J/kT) + 10\exp(6J/kT)]/[1 + 3\exp(2J/kT) + 5\exp(6J/kT)]$$

$$\chi_{mono} = 2Ng^2\mu_B{}^2/3kT$$

$$R = \Sigma(\chi^{calc} - \chi^{obs})^2/\Sigma(\chi^{obs})^2$$

(20) Chauduri, P.; Küppers, H.-J.; Wieghardt, K.; Gehring, S.; Haase, W.; Nuber, B.; Weiss, J. *J. Chem. Soc., Dalton Trans.* **1988**, 1367.

(21) Sacconi, L.; Mani, F.; Bencini, A. In *Comprehensive Coordination Chemistry*; Wilkinson, G., Ed.; Pergamon: Oxford, 1987; Vol. 5, p 56.

(22) (a) Casabó, J.; Pons, J.; Siddiqi, K. S.; Teixidor, F.; Molius, E.; Miravittles, C. *J. Chem. Soc., Dalton Trans.* **1989**, 1401. (b) Storr, A.; Summers, D. A.; Thompson, R. C. *Can. J. Chem.* **1998**, *76*, 1130.

(23) (a) Ajò, D.; Bencini, A.; Mani, F. *Inorg. Chem.* **1988**, *27*, 2437. (b) Nishida, Y.; Kida, S. *Inorg. Chem.* **1988**, *27*, 447. (c) Hanot, V. P.; Robert, T. D.; Kolnaar, J.; Haasnoot, J. G.; Reedijk, J.; Kooijman, H.; Spek'l, A. L. *J. Chem. Soc., Dalton Trans.* **1996**, 4275. (d) Matsushima, H.; Hamada, H.; Watanabe, K.; Koikawa, M.; Tokii, T. *J. Chem. Soc., Dalton Trans.* **1999**, 971.

Table 9. Results of the Ethanolysis of Urea: Formation of Ethyl Carbamate after 6 Days

compd	equiv of ethyl carbamate
1	0.8 ± 0.2
2b	0.8 ± 0.2
3a	0.0
4	2.2 ± 0.2
$HL^1/2[Ni(H_2O)_6](ClO_4)_2$	1.1 ± 0.2
$HL^2/2[Ni(H_2O)_6](ClO_4)_2$	0.0

present discussion).[18] Nonlinear fits of the experimental data to eq 1 (not including a paramagnetic impurity) yield the parameters listed in Table 8. Comparing these values with those obtained for **1** and **2a**, a trend of decreasing J with increasing metal−metal separation transpires. However, the only marginal superexchange found for the asymmetric complex **3a** contrasts the previously reported substantial increase of the antiferromagnetic coupling that occurs when an OC-6 species transforms to a SPY-5 species in a series of doubly phenoxide bridged dinickel(II) compounds,[24] while the difference in J for **2a** and **3a** is in good agreement with the analogous trend observed for the related symmetric and asymmetric Cl-bridged complexes.[10] In the case of **4a** an extrusion of MeOH solvent molecules from the crystals upon preparation of the sample for magnetic measurement (powdering and drying under vacuum) has to be assumed, so that a conservation of the dinuclear structure as deduced from single-crystal X-ray crystallography is questionable and we thus abstain from further interpretation of the data.

Ethanolysis of Urea. In conjunction with the search for functional models of urease, a catalytic conversion of urea into ethyl carbamate[8] as well as the stoichiometric degradation of urea to the cyanate ion[6g,9b] has been reported for dinuclear nickel(II) systems. We have now studied the ethanolysis of urea with the present new complexes in order to evaluate their ability to function as model systems for urease.

In a typical experiment, an ethanol solution containing the respective species **1**, **2b**, **3a**, or **4** (1.7 mM), 30 equiv of urea, and inert 1,3,5-trimethoxybenzene (3.3 mM) as an internal standard was stirred under reflux for 6 days. In the absence of any dinickel complex or if only $[Ni(H_2O)_6](ClO_4)_2$ is present, no formation of ethyl carbamate can be observed under these conditions. On the other hand, the action of the above complexes gives rise to the formation of ethyl carbamate in some cases, as analyzed by ^{1}H NMR spectroscopy and summarized in Table 9.

1 and **2b** do hardly show stoichiometric activity (expectedly being equal for both systems), the conversion of urea amounting to only 0.8 ± 0.2 equiv (with respect to the complex employed). The asymmetric species **3a** turns out to be completely inactive, whereas **4** displays a more pronounced activity and yields 2.2 ± 0.2 equiv of the product ethyl carbamate after 6 days.

Obviously the presence of only one accessible coordination site at the dinuclear core as seen for **3a** is insufficient for allowing solvolysis of urea, in accord with the idea of a requisite binding and activation of both the substrate and the nucleophile at the two nickel centers.[4,5] While this latter condition may be met in **1** and **2b**, the unfavorable stereochemical orientation of the two remote exo binding sites in these cases appears to be inappropriate for a subsequent intramolecular attack of the nucleophile on the bound substrate, and hence the yield of ethyl carbamate is very low. For comparison, we also employed a simple mixture of HL^1 and 2 equiv of $[Ni(H_2O)_6](ClO_4)_2$ under identical experimental conditions (Table 9), giving rise to a slight increase in activity compared to **1** and **2b**. However, the identity of the corresponding active complex lacking a bridging acetate remains elusive. A mixture of asymmetric HL^2 and 2 equiv of $[Ni(H_2O)_6](ClO_4)_2$ turns out to again be inactive. The presence of several potentially available docking sites for the reactants as in **4** clearly enhances the potential of the dinickel system to mediate the solvolysis of urea, even though the observed activity is still very low. The only other two dinickel(II) complexes that have been reported to catalyze the ethanolysis of urea accomplished a conversion of 4.1 or 2.05 equiv after 12 h reflux in ethanol.[8] In those systems a dinucleating alkoxide ligand and a secondary acetate or hydrogen carbonate bridge, respectively, provide an overall coordination environment that leaves one accessible site at each metal ion, where these sites are oriented in a favorable cis arrangement with respect to the bimetallic core and thus enable a more suitable positioning of the reactants urea and ethanol. Considering the many labile ligands in **4**, it should be emphasized that a one-metal mechanism in which solely the two adjacent coordination sites at a single metal ion are involved in the solvolysis reaction is likely and cannot be ruled out for this complex. This latter possibility is particularly feasible in light of the various hydrolytic reactions enabled by some related mononuclear complexes that feature two cis-arranged active coordination sites at a single metal ion.[25]

Conclusions

A series of pyrazolate-based dinuclear nickel(II) complexes with secondary acetate bridges and accessible coordination sites proved suited for binding urea, where this substrate is linked to the bimetallic core via synergetic O-coordination and H-bridging between suitable urea amino groups and O atoms of the acetate bridges. The general ability of the bridging acetate to contribute to the association of additional entities with such dinuclear complexes is further underlined by the incorporation of a sodium ion in **5**. The magnetic superexchange observed for the (μ-pyrazolato)(μ-acetato)dinickel(II) framework is weakly antiferromagnetic, and a correlation with the tilting of the acetate moiety with respect to the plane of the pyrazolate as well as with the Ni···Ni distance transpires. The differing ability of these complexes to induce ethanolysis of urea is related to the number and stereochemical arrangement of the accessible coordination sites available for substrate binding, in accord with the basic concept of the widely accepted mechanism of urease activity.[4,5] However, the properties of the sole new dinickel complex that shows a distinct (although very low) activity for the solvolysis reaction, i.e., **4**, may also be related to the presence and cooperative action of two adjacent cis coordination sites at each individual metal center.

Acknowledgment. We are grateful to Prof. Dr. G. Huttner for his generosity and his continuous interest in our work as well as to the Deutsche Forschungsgemeinschaft and the Fonds der Chemischen Industrie for fellowships and financial support.

Supporting Information Available: Listings of crystallographic data, positional and thermal parameters, and interatomic distances and angles for **1**, **2c**, **3a**, **4**, and **5**; representative NMR traces of the ethanolysis reactions by **1** and **4** (Figures S1 and S2, respectively). This material is available free of charge via the Internet at http://pubs.acs.org.

IC990137U

(24) (a) Nanda, K. K.; Das, R.; Thompson, L. K.; Venkatsubramanian, K.; Paul, P.; Nag, K. *Inorg. Chem.* **1994**, *33*, 1188. (b) Nanda, K. K.; Thompson, L. K.; Bridson, J. N.; Nag, K. *J. Chem. Soc., Chem. Commun.* **1994**, 1337.

(25) See, for example: (a) Breslow, R.; Fairweather, R.; Keana, J. *J. Am. Chem. Soc.* **1967**, *89*, 2135. (b) Chin, J.; Kim, J. H. *Angew. Chem. Int. Ed. Engl.* **1990**, *102*, 580; *Angew. Chem., Int. Ed. Engl.* **1990**, *29*, 523. (c) De Rosch, M. A.; Trogler, W. C. *Inorg. Chem.* **1990**, *29*, 2409.